September 1986
LU TP 86-17
UCLA-86-002

PYTHIA: The Lund Monte Carlo for Hadronic Processes*

Hans-Uno Bengtsson
Department of Physics
UCLA, 405 Hilgard Avenue
Los Angeles, California 90024, USA

and

Torbjörn Sjöstrand
Department of Theoretical Physics,
University of Lund, Sölvegatan 14A,
S-223 62 Lund, Sweden

Abstract:
PYTHIA is a Monte Carlo program intended for the study of high-p_T physics in hadronic interactions, but also covers the domain of low-p_T interactions as an integral part of the total cross-section. In its present form, version 4.7, it includes matrix elements for the basic $2 \to 1$ and $2 \to 2$ standard model (strong and electroweak) subprocesses (as well as some non-standard model subprocesses), elastic and diffractive scattering, multiple interactions, structure functions and initial and final state parton showers.

*to appear in the proceedings of the 1986 Summer Study on the Physics of the Superconducting Super Collider, Snowmass, Colorado, June 23 - July 11, 1986

PYTHIA: THE LUND MONTE CARLO FOR HADRONIC PROCESSES

H.-U. Bengtsson
Department of Physics, UCLA, 405 Hilgard Avenue, Los Angeles, California 90024
and
T. Sjöstrand
Department of Theoretical Physics, University of Lund, Sölvegatan 14 A, S-223 62 Lund, Sweden

Summary

PYTHIA is a Monte Carlo program intended for the study of high-p_T physics in hadronic interactions, but also covers the domain of low-p_T interactions as an integral part of the total cross-section. In its present form, version 4.7, it includes matrix elements for the basic $2 \to 1$ and $2 \to 2$ standard model (strong and electroweak) subprocesses (as well as some non-standard model subprocesses), elastic and diffractive scattering, multiple interactions, structure functions and initial and final state parton showers.

Introduction

When word had reached king Crœsus that Astyages had been deposed by Cyrus, Cambyses' son, and that the Persian empire was every day growing stronger, he turned his thoughts from domestic troubles to warfare and resolved to ask an oracle what the outcome would be in a potential battle against the powerful usurper. However, to have some guarantee for the value of the prophecy, he first sent embassies to the most renowned oracles: to Delphi and to Abæ in Phocis, to Dodona, Amphiaraus and Trophonius, to the Branchidæ of Miletus and to Ammon's temple in Libya. The messengers were instructed to inquire of the different divinities on the hundredth day after their departure from Sardis what Crœsus, Alyattes' son, king of the Lydians, was doing at that precise moment, and to record the answers carefully and bring them back to their ruler. What Crœsus had ordered was accordingly done, and when the messengers returned, the king could promptly discard all oracles but one — the one that had been murmured by a fuddled sibyl from the tripod at the magic crevice in Delphi, been put into verse by the priests of Apollo, announcing in laboured hexameters:

οἶδα δ' ἐγὼ ψάμμου τ' ἀριθμὸν καὶ μέτρα θαλάσσης,
καὶ κωφοῦ συνίημι, καὶ οὐ φωνεῦντος ἀκούω.
ὀδμή μ' ἐς φρένας ἦλθε κραταιρίνοιο χελώνης
ἑψομένης ἐν χαλκῷ ἅμ' ἀρνείοισι κρέεσσιν,
ἦ χαλκὸς μὲν ὑπέστρωται, χαλκὸν δ' ἐπιέσται.

[*I know the number of grains of sand as well as the expanse of the sea,*
And I comprehend the dumb and hear him who does not speak.
There came to my mind the smell of the hard-shelled turtle,
Boiled in copper together with lamb,
With copper below and copper above.]

The veracity of the Pythia had thus been established beyond all doubt by the crafty ruler who, according to Herodotus,[1] had waited for the appointed day, slaughtered a turtle and a lamb, and boiled them together in a copper cauldron with a copper lid.

The history of PYTHIA, The Lund Monte Carlo for Hadronic Processes, is neither as long nor as dignified as that of its eponym. The first published version, 2.2,[2] was a simple attempt to simulate the essentials of quark and gluon interactions at ISR energies. It included the fundamental $2 \to 2$ QCD subprocesses, but used a constant α_S and scaling structure functions; beam and target particles contained valence quarks and gluons only. The simulation was improved in the next version, 3.4,[3] which introduced a running α_S and standard parametrizations of scale breaking structure functions; the basic processes still remained the same, however. With the advent of data from the CERN $\bar{p}p$-collider it became clear that in order to get a reasonable description of real events, initial and final state radiation would have to be taken into account. Furthermore, following the publication of data on e.g. W^+ and Z^0 production, there has been an increased interest in accurate simulation of general standard model processes. The projected Superconducting Supercollider (SSC) will presumably be able to probe more of the structure of the standard model, including the still elusive Higgs. These considerations prompted the development of an almost entirely new Monte Carlo program for hadron-hadron collisions. Included is a next to complete set of basic standard model hard processes (and some non-standard model ones), as well as 'minimum bias' physics, i.e. low-p_T events, diffractive scattering and elastic scattering. The resulting program, PYTHIA version 4.7,[4] is now available for general use.

Basic Hard Scattering

At the core of all present Monte Carlo programs devoted to high-p_T physics lie the matrix elements of the simple $2 \to 2$ subprocesses. (It is true that exact cross-sections for the $2 \to 3$ subprocesses and the associated virtual corrections to the $2 \to 2$ subprocesses have now been calculated,[5] but a Monte Carlo implementation of these, if combined with shower algorithms for multi-jets, runs into problems of double counting.) The cross-sections $\hat{\sigma}(\hat{s}, \hat{t}, \hat{u})$ for the $2 \to 2$ hard scatterings are convoluted with structure functions incorporating leading-log scaling violations to form a total cross-section σ for the subprocess, i.e.

$$\sigma = \sum_{i,j,k} \iiint d\tau dx_F d\hat{t}\, \hat{\sigma}^k_{ij}(\hat{s}, \hat{t}, \hat{u}) f^1_i(x_1, Q^2) f^2_j(x_2, Q^2), \quad (1)$$

where i and j give the partons from particles 1 and 2, respectively, k specifies the final state (when a given initial state can lead e.g. to different final state colour configurations; see below), and we have used the standard definitions

$$\begin{aligned} \tau &\equiv x_1 x_2, \\ x_F &\equiv x_1 - x_2. \end{aligned} \quad (2)$$

PYTHIA 4.7 includes practically all $2 \to 2$ subprocesses possible in the standard model, i.e. quark and gluon scattering, resonance production of Z^0/γ^*, $W^\pm$ and H^0 (the latter from WW and ZZ fusion, as well as from the more conventional gg and $q\bar{q}$ reactions), pair production of gauge bosons, and production of one gauge boson plus a quark or a gluon jet (cf. Table

1). Quarks are generally treated as massless in the matrix elements; an obvious exceptions is e.g. the reaction $q + \bar{q} \to H^0$, where the coupling is proportional to $(m_q/m_H)^2$ and a neglect of the quark masses would have rather disconcerting results. All possible standard model decays of the resonances are implemented, and specific decay product flavours can be chosen for each resonance separately. Furthermore, the allowed recoiling quark flavours q' (q'', q''') in the reactions $g + q \to q' + W^\pm$ ($[q + q' \to q'' + q''' +] W^+ + W^- \to H^0 [+ q'' + q''']$) can also be chosen separately, as can the initial flavours entering the hard scattering for any subprocess.

Table 1: Partonic Subprocesses in PYTHIA 4.7

$q_i(\bar{q}_i) + q_j(\bar{q}_j) \to q_i(\bar{q}_i) + q_j(\bar{q}_j)$	$q_i + \bar{q}_i \to \gamma + Z^0$
$q_i + \bar{q}_i \to q_k + \bar{q}_k$	$q_i + \bar{q}_j \to \gamma + W^\pm$
$q_i + \bar{q}_i \to g + g$	$q_i + \bar{q}_i \to Z^0 + Z^0$
$q_i(\bar{q}_i) + g \to q_i(\bar{q}_i) + g$	$q_i + \bar{q}_j \to Z^0 + W^\pm$
$g + g \to q_k + \bar{q}_k$	$q_i + \bar{q}_i \to W^+ + W^-$
$g + g \to g + g$	$q_i + \bar{q}_i \to H^0$
$q_i + \bar{q}_i \to Z^0/\gamma^*$	$g + g \to H^0$
$q_i + \bar{q}_j \to W^\pm$	$Z^0 + Z^0 \to H^0$
$g + q_i(\bar{q}_i) \to \gamma + q_i(\bar{q}_i)$	$W^+ + W^- \to H^0$
$g + q_i(\bar{q}_i) \to Z^0 + q_i(\bar{q}_i)$	$q_i + \bar{q}_i \to H^0 + Z^0$
$g + q_i(\bar{q}_i) \to W^\pm + q_j(\bar{q}_j)$	$q_i + \bar{q}_j \to H^0 + W^\pm$
$q_i + \bar{q}_i \to g + \gamma$	$q_i + \bar{q}_j \to R$
$q_i + \bar{q}_i \to g + Z^0$	$q_i + \bar{q}_j \to H^\pm$
$q_i + \bar{q}_j \to g + W^\pm$	$q_i + \bar{q}_i \to Z'^0/Z^0/\gamma^*$
$q_i + \bar{q}_i \to \gamma + \gamma$	

In the production of a single resonance, the mass is chosen according to the proper cross-section, i.e. the basic Breit-Wigner shape folded with the structure functions. Since the latter are falling with x, the high-mass tail of the resonance is in general suppressed, whereas the low-mass tail is significantly enhanced. Indeed, a secondary peak in the cross-section may appear for $m \to 0$. The minimum mass can be selected by the user to avoid the generation of undesirable events. Decays are into the channels allowed by the user, according to conventional mass dependent branching ratios, and with the correct angular distribution; for the Z^0/γ^* this means the implementation of the full interference structure and forward-backward correlations.

Resonances produced in $2 \to 2$ processes are assumed to be on mass-shell; optionally a symmetric Breit-Wigner shape may be obtained. Further, the full Z^0/γ^* coupling is not here implemented in the production of a Z^0. In the decay of resonances, the angular distribution is chosen according to the correct matrix elements.[6] These matrix elements are of the $2 \to 4$ type for the production of a pair of resonances and of the $2 \to 3$ type for a single resonance recoiling against a q, a g, or a γ. Correct angular distributions are also included for the decay chain $H^0 \to Z^0Z^0$, $W^+W^- \to 4$ fermions.

It will be noted that Table 1 in addition contains some non-standard processes, namely the production of a heavy flavour-changing neutral boson, R, as proposed by Hou and Soni,[7] the production of a charged Higgs, $H^\pm$, as suggested in minimal extensions of the standard model,[8] and the production of a new electroweak gauge boson Z'^0, as implied by superstring theories.[9] This latter subprocess has been implemented with the full $Z'^0/Z^0/\gamma^*$ interference structure included. A further non-standard model possibility incorporated into PYTHIA 4.7 is the decay channel $Z^0/\gamma^* \to H^+ + H^-$. Apart from being interesting reactions in their own rights, these subprocesses also serve as examples of how other non-standard processes can be implemented into the program by the enterprising user.

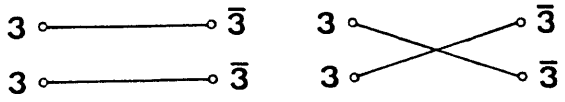

Fig. 1. A partonic system of two colour triplets and two colour antitriplets and the corresponding two possible colour field topologies.

The cross-sections for all the above subprocesses are readily available in the literature.[7,8,10] However, since PYTHIA is designed to set up a partonic system that can eventually be hadronized by string fragmentation, some care needs to be exercised. As will be explained below, the string representing a colour flux tube is spanned according to the ordering in colour space of the coloured partons, quarks and gluons. A simple partonic system consisting e.g. of two colour triplets (quarks, say) and two colour antitriplets (antiquarks, say) already admits of two entirely different string configurations when colour singlet systems are to be formed (see Fig. 1). If hadrons are produced by subsequent breakups along the strings, these different colour field topologies translate into different final state hadron distributions, which (at least in principle) should be experimentally distinguishable. This will be true not only of string fragmentation, but of any essentially longitudinal fragmentation model that respects fundamental colour ordering, such as cluster fragmentation. The situation becomes event more complicated with the introduction into the partonic system of one or more gluons (colour octets): a given subprocess can now give rise to several different colour field topologies with very different properties as to the final state hadron distributions. As an example, the reaction $q + g \to q + g$ which has contributions from the three Feynman diagrams in Fig. 2 contains two different colour flows (Fig. 3): either from 1 to 2 to 3 to 4 (a) or from 1 to 3 to 2 to 4 (b). These colour flows translate into the colour field configurations of Fig. 4. (For this reaction the experimental consequences of the two different colour field topologies have recently been studied, and an observable capable of distinguishing between them been constructed.[11]) What is needed then is the cross-section for a specific colour configuration rather than for a specific subprocess. In many cases these two amount to the same thing; processes like $q + \bar{q}' \to W^\pm$, e.g., where the final state is a colour singlet, admit of only one colour topology (a string spanned between the remnants of the two hadrons from which the quark and the antiquark have scattered), and the cross-section for the colour configuration is thus identical to the cross-section for the subprocess as a whole. As gleaned from the above, however, this is in general not true for the pure QCD processes, and a recipe is needed for calculating the cross-sections of the different colour topologies. It has been shown[12] that QCD processes can be formulated in a gauge-invariant way in terms of colour flows,

for which a set of 'Feynman rules' can be given. Using these rules, the amplitude for any colour flow can be written down and contact be made with the normal Feynman diagrams by inspection of the colour content of their corresponding amplitudes. In this fashion the desired cross-sections can be calculated; when summed over different colour flows, the standard cross-sections for the QCD subprocesses are regained (except for possible interference terms). These calculations were carried out already for the earliest version of PYTHIA and can be found in ref. 3, together with the set of rules necessary for the mathematical interpretation of colour flow diagrams. The results are fully implemented in PYTHIA 4.7. (It should perhaps be noted that although a straightforward treatment would seem to preclude the existence of interference terms between different colour flows belonging to the same subprocess — and consequently in some instances lead to a different cross-section from the one obtained by standard QCD calculations —, PYTHIA contains options for running both with and without the inclusion of these interference terms in the matrix elements. Also, in conjunction with independent fragmentation which does not respect colour flows, the division of the cross-section of a subprocess on different colour topologies of course has no meaning.)

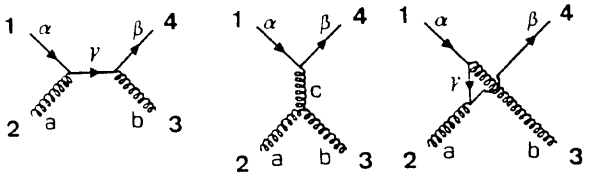

Fig. 2. The three Feynman diagrams contributing to the process $q + g \to q + g$.

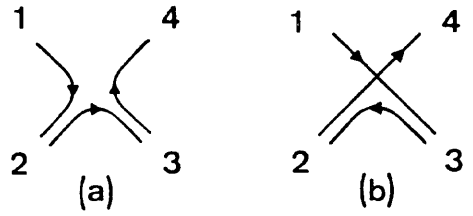

Fig. 3. The two possible colour flows of the process $q + g \to q + g$.

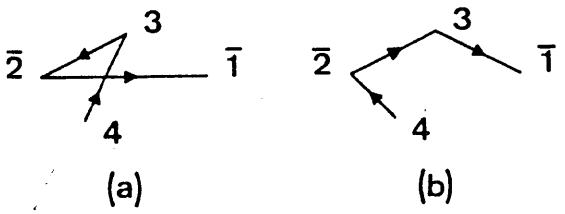

Fig. 4. The two string configurations corresponding to the two colour flows in fig. 2. $\bar{1}$ and $\bar{2}$ denote the remnants in colour space of hadrons 1 and 2, respectively, after partons 1 and 2 have scattered.

The options for structure functions include the parametrizations of Eichten, Hinchliffe, Lane and Quigg,[10] Duke and Owens,[13] and Glück, Hoffman and Reya[14] for the proton, and Owens[15] for the pion. A further possibility recently implemented is the use of the structure function evolution program of Wu-Ki Tung[16] which can be run from PYTHIA at intialization.

This completes the survey of the basic $2 \to 2$ subprocesses. As a demonstration of its capabilities, we show in Fig. 5 results obtained using PYTHIA 4.7 to generate the signal (a high mass $e^{\mp}\mu^{\pm}$ pair) from production of a horizontal gauge boson R at the SSC, as well as the background (from e.g. W^+W^- pair production)[17].

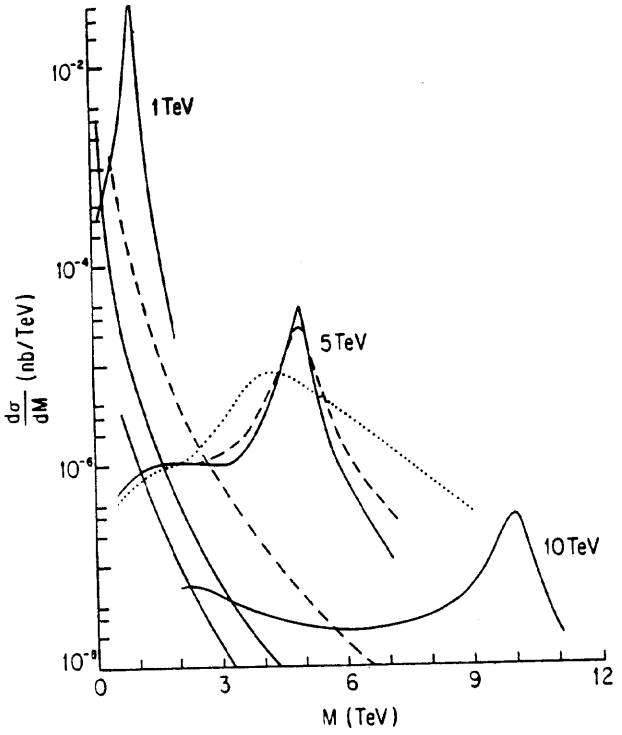

Fig. 5. A plot of $d\sigma/dM$ vs. M (where M is the invariant mass of the lepton pair) for the leptonic decays of a horizontal gauge boson R of masses 1, 5 and 10 TeV/c^2. For $m_R = 5\ TeV/c^2$, effects of different types of energy smearing are plotted as dotted and dashed curves. Also shown are the backgrounds from WW decays to $e\mu$ (solid curves; the upper corresponds to no p_T cuts, the lower to a p_T cut of 200 GeV/c on e and μ separately), and the Drell-Yan production of e^+e^-, $\mu^+\mu^-$ and $\tau^+\tau^-$ (dashed curve). (Figure taken from ref. 17.)

Apart from the hard scattering subprocesses, PYTHIA 4.7 can also generate 'genuine' low-p_T events (in addition to the minimum bias events from multiple hard and semi-hard scatterings discussed below), which are treated as the exchange of zero-energy gluons, and events with elastic as well as single and double diffractive scattering. These latter processes have the same general structure: t, the momentum transfer between the incoming hadron and the outgoing system (a hadron or an excited state), is given by a distribution

$$\exp(Bt + Ct^2)dt, \tag{3}$$

where B is the nuclear slope parameter and C the curvature parameter. For each diffractive system an additional factor dM^2/M^2 is multiplied on to give the mass M of the excited state. The diffractive system is subsequently treated as a string with the quantum numbers of the original hadron. Since the exact nature of the 'pomeron' exchanged between the hadrons is unknown, two alternatives are included. In the first, the

pomeron is assumed to couple to (valence) quarks, so that the string is stretched directly between the struck quark and the remnant diquark (antiquark) of the diffractive state. In the second, the interaction is rather with a gluon, giving rise to a 'hairpin' configuration in which the string is stretched from a quark to a gluon and then back to a diquark (antiquark). The total hadronic cross-section and the elastic cross-section, as well as the nuclear slope parameter B, are calculated using the parametrizations of Block and Cahn;[18] for the diffractive cross-sections the ansatz of Goulianos[19] is used. The curvature parameter C is found from a simple parabola fit to the values at different energies calculated by Block and Cahn in the Chou-Yang model,[20] incorporating also the value of $C \approx 5\,(\mathrm{GeV})^{-4}$ measured at the ISR.

Initial and Final State Radiation

The previous section dealt with hard $2 \to 2$ (or $2 \to 1$) processes. The cross-sections for these processes are obtained by applying lowest order perturbation theory; thus higher order corrections are, at this point, unaccounted for. In principle perturbations should be calculated both with respect to QCD and QFD ($SU(2) \times U(1)$) corrections. As an example, if the lowest order process is $q+g \to q+g$, then processes in the next order include $q+g \to q+g+g, q+g \to q+q'+\bar{q}', q+g \to q+g+\gamma$, $q+g \to q+g+Z^0$ and $q+g \to q'+g+W^{\pm}$. In the same order, there will also be loop corrections to the $q+g \to q+g$ matrix element; these corrections are needed in order to cancel soft and collinear divergences in the $2 \to 3$ processes.

In practice, one can often neglect the QFD corrections, but never the QCD ones. There are two reasons for the latter point: firstly, the strong coupling constant α_S is large, and secondly, by virtue of having incoming hadrons, all hard processes must involve coloured partons. By contrast, α_{em} is much smaller, and a graph like $g+g \to g+g$ does not contain any charged particles at all. The interest in QFD corrections is therefore more process-specific: contributions from $q+g \to q'+g+W^{\pm}$ are negligible when seen as just another source of high-p_T jets, but not necessarily so when studying the probability of finding a W in conjunction with extra high-p_T jets. As of yet, no QFD corrections have been included in PYTHIA, except for the well-known shift of W and Z masses. The following will therefore deal exclusively with QCD corrections.

By now, all graphs of order α_S^3 have been calculated, i.e. all $2 \to 3$ processes including virtual corrections to $2 \to 2$ ones.[5] Additionally, many $2 \to 4$ results are available,[21] but here without any study of virtual corrections to the same order. Already at present energies, events with four or more well separated high-p_T jets are legio, and most of these jets actually have (we believe) a subjet structure that is not experimentally resolvable but does affect properties like charged multiplicities and transverse momenta. At higher energies, like the SSC, this will be even more true. It was therefore decided to forego a matrix element approach in favour of a parton cascade picture, where the emission of an arbitrary number of partons is automatically included. The price to be paid is a less accurate representation of the cross-section for well separated jets, where the result from showers could easily deviate from the 'true' matrix element answer by factors of two or more. It may be possible to find schemes for trying to correct this discrepancy,[22] but this has not so far been carried out.

In the parton shower approach, one distinguishes between initial state radiation and final state radiation. In general, such a separation is not possible, because of the presence of interference terms. However, bremsstrahlung close to the directions of the two incoming partons (in the basic $2 \to 2$ process) is obviously dominated by the collinear divergences from initial state radiation graphs, and correspondingly final state radiation dominates close to the directions of the two outgoing partons. The neglect of interference terms should therefore not be crucial in the important regions.

Initial and final state radiation are in the following considered separately: although they share a common structure, the details are actually quite different.

Final State Radiation

Final state parton showers are timelike: all partons have $m^2 \geq 0$. The evolution is based on an iterative use of the branchings $q \to qg$, $g \to gg$ and $g \to q\bar{q}$, as given by the Altarelli-Parisi evolution equations:[23]

$$\frac{dP_{a\to bc}}{dt} = \frac{\alpha_S(Q^2)}{2\pi} \int dz P_{a\to bc}(z). \tag{4}$$

Here z gives the sharing of energy (or some combination of energy and momentum) between the daughters b and c, and t is the evolution parameter; usually $t = \ln(m_a^2/\Lambda^2)$. The Altarelli-Parisi splitting kernels $P_{a\to bc}(z)$ are

$$\begin{aligned} P_{q\to qg}(z) &= \frac{4}{3}\frac{1+z^2}{1-z} \\ P_{g\to gg}(z) &= 6\frac{[1-z(1-z)]^2}{z(1-z)} \\ P_{g\to q\bar{q}}(z) &= \frac{1}{2}[z^2+(1-z)^2] \end{aligned} \tag{5}$$

(where an additional factor $\frac{1}{2}$ for identical particles should be included when integrating $P_{g\to gg}(z)$).

Starting at the maximum allowed mass for parton a, t may be successively degraded until a branching occurs. The products b and c may be allowed to branch in their turn, and so on. The parton branching is stopped when a parton mass is evolved below some minimum value, i.e. $t < t_{min} = \ln(m_{min}^2/\Lambda^2)$. (Obviously, allowances have to be made for quark masses, in particular for heavy flavours.) The probability that a parton does not branch between some initial maximum t and t_{min} is given by the Sudakov form factor

$$S_a(t) = \exp\left[-\int_{t_{min}}^{t} dt' \frac{\alpha_S(Q'^2)}{2\pi} \int dz P_{a\to bc}(z)\right]. \tag{6}$$

The probability distribution $P_a(t_{max}, t)$ that a parton a with maximum allowed virtuality t_{max} will actually obtain the virtuality t is then

$$P_a(t_{max}, t)dt = S_a(t_{max})\frac{d}{dt}\left(\frac{1}{S_a(t)}\right)dt. \tag{7}$$

The exact choice of z and t definition in practice plays an important rôle for the detailed nature of the parton shower evolution. Several different algorithms are documented in the literature.[24,25,26] In particular, the Marchesini-Webber model[26] includes coherence effects[27] by a suitable choice of evolution parameter. In JETSET 6.2 two algorithms are included, one conventional (incoherent) à la Kajantie-Pietarinen and one coherent à la Marchesini-Webber; in neither case do we guarantee exact equivalence with the originals (see ref. 28 for details). In principle, the coherent algorithm is the theoretically most reliable one and is obtained by default, but it is useful to have

different options available. In the upcoming JETSET 6.3 version, the showering algorithm has been rewritten so as to obtain or not obtain the angular ordering required by coherence without affecting any other parts of the algorithm.[29]

The evolution equations contain $\alpha_S(Q^2)$, and thus depend on the choice of Q^2 scale. Studies of coherence effects[29] suggest that the p_T^2 of the daughters b and c should be more relevant than the more obvious choice m_a^2. As default option we therefore have $Q^2 = z(1-z)m_a^2 \approx p_T^2$, but leave $Q^2 = m_a^2/4$ as another choice.

Now for some details specific to applications of final state radiation in hadron physics. The two outgoing partons are always boosted to their CM frame and evolved there (in the coherent algorithm, a special frame with 90° opening angle between the two partons is used in intermediate steps), and in this frame the total energy is also preserved during the shower evolution (or afterwards, by rescaling, in the coherent option). Thus, in a process like $q + g \to q + \gamma$, if the final q acquires a mass, the p_T (and p) of the γ is reduced accordingly. The maximum virtuality Q^2_{max} is by default chosen to be $4p_T^2$, with p_T the scale of the hard $2 \to 2$ interaction. Thus, for a 90° scattering, $Q^2_{max} = \hat{s}$, which is the same value that is allowed e.g. in final state evolution in W and Z decays. On the other hand, $Q^2_{max} \to 0$ for scatterings with $p_T \to 0$, event if the $\hat{s}$ of the scatterings remains finite. The Λ value may be chosen separately, but it is by default taken to be the same as the one given by the choice of structure functions.

One test for the validity of the present approach is the recent UA1 study of quark and gluon jet fragmentation functions.[30] Agreement between model and data is here satisfactory (see e.g. Fig. 6).

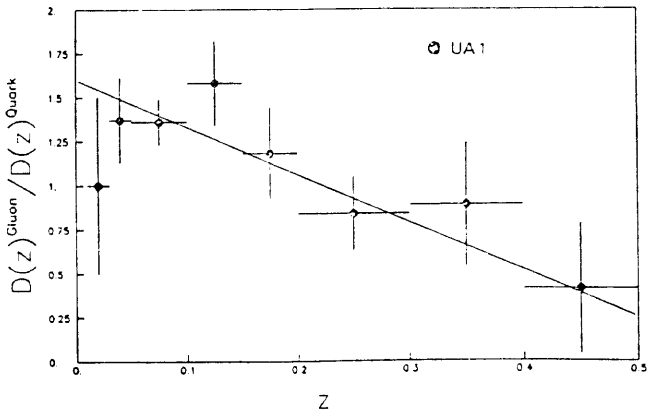

Fig. 6. Ratio of gluon to quark fragmentation functions: UA1 data points[30] compared with PYTHIA prediction, full line.

Initial State Radiation

A fast hadron may be viewed as a cloud of quasireal partons. At each instant, an individual parton can initiate a cascade, branching into a number of partons. These partons do not have enough energy to be on mass-shell, and thus only live for a finite time before reassembling. In a hard interaction between two incoming hadrons, when two partons scatter to high p_T, also the other partons in the two related cascades are provided with the necessary energy to live indefinitely. For Monte Carlo applications, it is convenient to imagine that the full spacelike virtuality, $m^2 < 0$, $Q^2 \approx -m^2 > 0$, is carried by the two interacting partons. Then the momentum transfer given by the central $2 \to 2$ hard scattering subprocess is enough to ensure that all partons of the two related cascades may end up on mass shell.

In principle, the evolution of a cascade could be carried out from the cascade intiating parton at a low Q^2 scale to the incoming parton at the hard interaction, i.e. forward in time.[31,32] There are a number of problems associated with this approach, which have to do with the fact that the flavour, x and Q^2 values at the hard interaction are then not known until the very end of the evolution.[32] Instead, a 'backwards evolution' algorithm[33,34] has been developed, in which an already chosen hard scattering forms the starting point. The evolution is then reconstructed step by step in falling Q^2 sequence back towards the shower initiators. An analogue to the Sudakov form factor, eq. (6), may be constructed as follows.

The Q^2 evolution of partons inside a cascade is again given by the Altarelli-Parisi equations; if written for the structure functions they take the form

$$\frac{df_b(x,t)}{dt} = \frac{\alpha_S(Q^2)}{2\pi} \sum_a \int \frac{dx'}{x'} f_a(x',t) P_{a\to bc}\left(\frac{x}{x'}\right). \quad (8)$$

Here $f_i(x,t)$ is the structure function for flavour i, x is the momentum fraction carried by a parton, and $P_{a\to bc}(z)$ are the splitting functions of eq. (5) (here without any symmetrization factor $\frac{1}{2}$ for the $g \to gg$ integral). The Altarelli-Parisi equations express the fact that during a small increase dt there is a probability for a parton a with the momentum fraction x' to become resolved into a parton b at $x = zx'$ and a parton c at $x' - x = (1-z)x'$. Correspondingly, during a decrease dt a parton b may be 'unresolved' into a parton a. The probability dP_b for this to happen is given by df_b/f_b which, using eq. (8), becomes

$$dP_b = \frac{df_b(x,t)}{f_b(x,t)} = |dt| \frac{\alpha_S(Q^2)}{2\pi} \sum_a \int \frac{dx'}{x'} \frac{f_a(x',t)}{f_b(x,t)} P_{a\to bc}\left(\frac{x}{x'}\right). \quad (9)$$

Summing up the cumulative effect of many small changes dt, the probability for no radiation exponentiates. Therefore one may define a form factor

$$S_b(x, t_{max}, t) = \exp\left[- \int_t^{t_{max}} dt' \frac{\alpha_S(Q'^2)}{2\pi} \sum_a \int \frac{dx'}{x'} \frac{f_a(x',t')}{f_b(x,t')} P_{a\to bc}\left(\frac{x}{x'}\right) \right] \quad (10)$$

giving the probability that a parton b remains at x from t_{max} to $t < t_{max}$. Implicit in S_b is also information on flavour, t and x values for the branchings that do occur (see ref. 33, 34 for details).

The reconstruction of the kinematics of the branchings is nontrivial. It depends, e.g., on the choice of interpretation of the $z = x/x'$ splitting variable. In this work, z is defined as the ratio of $\hat{s}$ values before and after a branching. Further, the parton c in the branching $a \to bc$ may be timelike, just like the two hard scattered partons, and give rise to a final state shower of its own, to be treated in the spirit of the previous subsection. Finally, the interpretation of t and Q^2 is ambiguous. The standard choice is $t = \ln(Q^2/\Lambda^2)$ with $Q^2 = -m^2/4$, but a wide selection of alternative definitions are available. For the phenomenology at present energies, uncertainties in these details do not seem to be particularly crucial for the outcome.[34] Like the evolution itself, the branchings are reconstructed with start at the hard $2 \to 2$ interaction, and with incoming partons along the $\pm z$ axis. As

each branching $a \to bc$ is considered, the event is rotated and boosted so that a becomes the one coming in along $+z$ or $-z$, rather than b.

Phenomenologically, this model seems to account well e.g. for the W/Z transverse momentum spectrum at SppS,[34] Fig. 7, and for the associated jet activity.

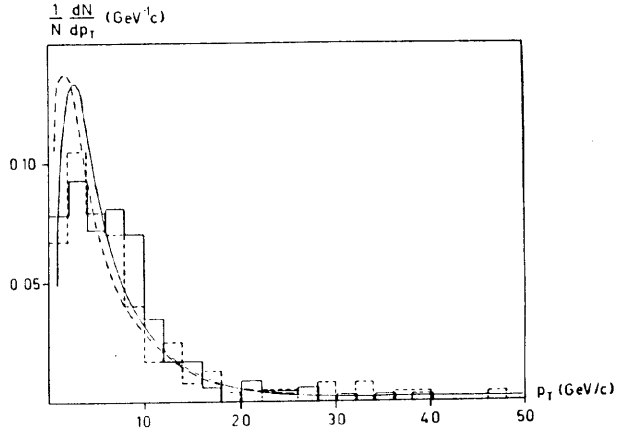

Fig. 7. W transverse momentum spectra. Histograms give experimental data, UA1 full and UA2 dashed.[35]

Beam Jets and Multiple Interactions

The differential cross-section for a parton-parton interaction is singular for the momentum transfer $\hat{t} \to 0$ (or $\hat{u} \to 0$), as expressed e.g. in the well-known rule of thumb that the p_T-spectrum for a parton from hard interactions should behave roughly like dp_T^2/p_T^4. The integrated cross-section of all interactions with $p_T > p_{T\,min}$, $\sigma_{hard}(p_{T\,min})$, is therefore divergent for $p_{T\,min} \to 0$. At present collider energies, $\sigma_{hard}(p_{T\,min})$ becomes comparable to the total cross-section for $p_{T\,min} \approx 1.5\,\mathrm{GeV/c}$. This need not lead to contradictions: $\sigma_{hard}(p_{T\,min})$ does not give the hadron-hadron cross-section but the parton-parton one. Each of the two incoming hadrons may be viewed as a beam of partons, with the possibility of several parton-parton interactions when the hadrons pass through each other, so that $\sigma_{hard} > \sigma_{tot}$ is perfectly allowed.

In ref. 36 it is argued that collider data indicate a significant probability for multiple interactions at 540 GeV. This conclusion is based on the assumption of jet universality, i.e. that the underlying fragmentation mechanism in hadron physics is no different from that in e^+e^- annihilation. With the string drawing described above, and if at most one hard interaction per event is allowed, the predicted multiplicity distribution is much narrower than the experimental one, and forward-backward correlations are almost absent.

If different parton interactions above $p_{T\,min}$ are assumed to take place (essentially) independently of each other, one obtains a Poissonian multiplicity distribution in the number of interactions, with mean given by $\sigma_{hard}(p_{T\,min})/\sigma_{tot}$, where σ_{tot} is the total inelastic, nondiffractive cross-section. With a varying number of interactions, the multiplicity fluctuations are increased, and strong forward-backward multiplicity correlations are introduced. Results are sensitive to the choice of $p_{T\,min}$ value (see Fig. 8), with a reasonable description obtained for $p_{T\,min} \approx 1.6\,\mathrm{GeV/c}$. Forward-backward multiplicity correlations, the rate of hot spots and other phenomena are also well described with this choice.

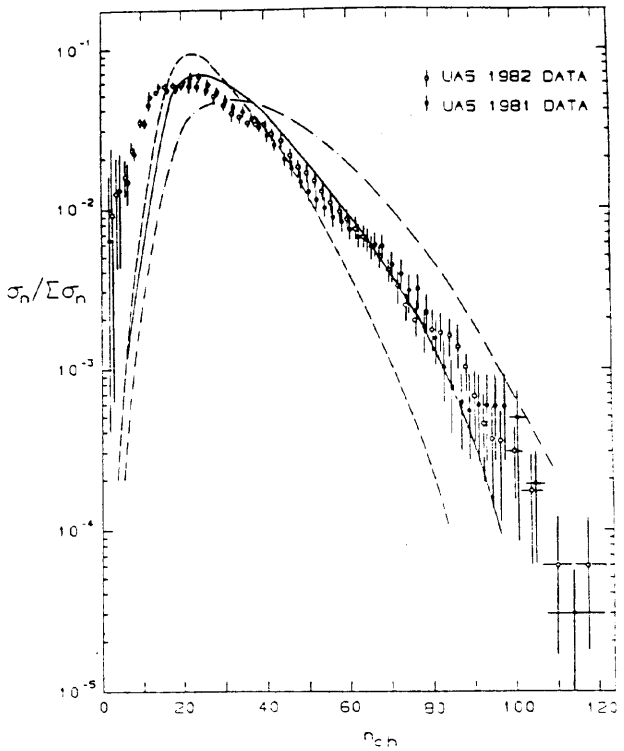

Fig. 8. Charged multiplicity distribution at 540 GeV: results from UA5[37] *vs. multiple interaction model. Dashed line: $p_{T\,min} = 2.0\,\mathrm{GeV/c}$; full line: $p_{T\,min} = 1.6\,\mathrm{GeV/c}$; dash-dotted line: $p_{T\,min} = 1.2\,\mathrm{GeV/c}$.*

The major free parameter of the model is thus the $p_{T\,min}$ cut-off scale. In a more realistic treatment a continuous turnover of the cross-section is expected, still with a characteristic scale of around 1.5 GeV. This can be understood as follows. The cross-section for the exchange of a single gluon between two incoming partons behaves like dp_T^2/p_T^4. However, an incoming hadron consists of a collection of partons with net colour charge zero. As smaller and smaller transverse momenta are considered, the wavelength of the exchanged gluon becomes larger and larger, the individual colour charges are no longer resolved, and therefore the cross-section does not increase as fast as naïvely expected.

A number of details remain to be discussed. If no interaction takes place above $p_{T\,min}$, it is assumed that a very soft $gg \to gg$ interaction still takes place, so that the colour flow is redirected. A 'low-p_T' event then consists of two strings, in pp collisions stretched between a diquark from one p and a quark from the other; in $p\bar{p}$ collisions one between diquark and antidiquark, and one between quark and antiquark. This provides a natural continuation to events above $p_{T\,min}$, where the dominant one-gluon exchange processes $qq' \to qq'$, $qg \to qg$ and $gg \to gg$ (with q valence quarks or antiquarks) have the same overall string drawing — in the last two processes with one or two extra intermediate gluons.

If two strings are stretched to a baryon remnant, it remains to be specified how the diquark and the quark share the remaining energy and momentum. With x representing the $E + p_L$ ($p_L = \pm p_z$ longitudinal momentum) fraction taken by the quark, a form

$$P(x)dx = \frac{(1-x)^3}{\sqrt{x^2+c^2}}dx \qquad (11)$$

is used. Here, $c = 2m_q/\sqrt{s} = 0.6\,\mathrm{GeV}/\sqrt{s}$ gives a cut-off of the singularity at $x = 0$. The shape has been chosen in rough agreement with the valence quark distribution, and seems to give sensible results, but it is by no means obvious.

Similar energy sharing distributions are needed when a sea quark is kicked out of the incoming hadron, producing a $qqqq$ or $qqq\bar{q}$ colour triplet remnant. In these cases the remnant is split into a hadron plus a remainder-jet: either a baryon plus a quark jet, or a meson plus a diquark jet. Flavours are paired taking into account that a sea $q\bar{q}$ pair comes from the splitting of a colour octet gluon so that, if one of them is kicked out, the other should end up in the hadron split off. Simple counting rules are used, based on the number of valence quarks in an object. Thus the x fraction of the quark jet or meson, respectively, is given by

$$P(x)dx = 2(1-x)dx. \tag{12}$$

For the generation of multiple interactions, the natural course is to start with the hardest interaction, i.e. the one with the highest p_T, and sequentially generate further interactions in falling p_T order, until $p_{T\,min}$ is reached.[36] In such a scheme, it is straightforward to have the hard interaction be any of the processes described above, with kinematics constrained as required by the user. Alternatively, the hard interaction can be just a normal QCD $2 \to 2$ process with the proper distribution for minimum bias events, including a fraction of events with no interactions at all above $p_{T\,min}$. Further, by having the interactions ordered, it is possible to take into account the energy carried away by preceding interactions, by letting the x obtained from structure functions always refer to remaining energy. This may be considered as the simplest possible approach to the complicated issue of defining simultaneous parton distribution functions.

The question of string drawing, nontrivial already when having only one hard scattering in an event, becomes even more ambiguous when several interactions are allowed. A few possibilities have been tried, with rather similar results; it is only the simplest of these that is obtainable in the present version of PYTHIA. Here the string drawing for the hardest interaction is handled as described above. All subsequent interactions are assumed to be of the $gg \to gg$ type; the full cross-section for QCD processes is used, however. Neither initial nor final state radiation is included. The two gluons are treated as if they were in a colour singlet state, i.e. a double string is spanned between them.

So far, it has been assumed that the initial state of all hadron collisions is the same, whereas in fact each collision is also characterized by a varying impact parameter b. A small b value corresponds to a large overlap between the two colliding hadrons, and hence an enhanced probability for multiple interactions. This may explain the 'pedestal effect', i.e. that events containing high-p_T jets also show above-average activity away from the jets. The status of these studies is described in ref. 38. The detailed description is not yet included in PYTHIA, but a simplified approach is, in which the probability for subsequent interactions is increased by a factor of two if the hardest interaction of the event has a large p_T value.

Fragmentation

The task of PYTHIA is to describe the partonic processes taking place in hadronic collisions. How these partons are transformed into the experimentally measurable particles, i.e. the process of fragmentation, is beyond its scope, at least in principle. With the information provided, PYTHIA could be combined with any well-defined fragmentation scheme. Of course, the most natural choice is to use the Lund Monte Carlo for jet fragmentation, JETSET version 6.2,[28] for which all the necessary interfaces are incorporated into PYTHIA.

Although independent fragmentation is included as an option, the standard fragmentation scheme of JETSET is the Lund string model.[39] This model takes as its starting point the belief that QCD is linearly confining at large distances. Now, the simplest Lorentz covariant and causal implementation of a linear potential is provided by the massless relativistic string. The mathematical string has no transverse extent, but the physical interpretation should rather be that the string coordinates parametrize the position of the axis of a cylindrically symmetric colour flux tube. The true nature of this tube need not be specified, but order-of-magnitude estimates give a flux tube radius of typical hadronic dimensions.

The endpoints of the string are associated with quarks and antiquarks, diquarks and antidiquarks. As a q (or $\bar{q}\bar{q}$) and a $\bar{q}$ (or qq) move apart, the potential energy stored in the intermediate string increases. The string may then break by the production of a new $q'\bar{q}'$ pair, so that the system splits into two colour singlet subsystems $q\bar{q}'$ and $q'\bar{q}$. If the invariant mass in either of these systems is large enough, further breaks may occur, and so on until only ordinary hadrons remain. Each of these hadrons is formed by the quark from one break and the antiquark from an adjacent break. Included is the production of pseudoscalar and vector mesons, and spin $\frac{1}{2}$ and spin $\frac{3}{2}$ baryons, most of which are unstable and decay further. The string breaking mechanism is understood as a tunnelling phenomenon, automatically providing a suppression of heavy flavour production and a Gaussian transverse momentum spectrum for primary hadrons.

The various $q'\bar{q}'$ breaks have a spacelike separation, i.e. they are causally disconnected. This spacelike separation implies that the time ordering of the breakup vertices is Lorentz frame dependent and hence irrelevant. It is therefore convenient to introduce an iterative procedure, in which the production closest to the ends is considered first, then the next closest ones, etc. The fraction z of remaining $E + p_L$ taken by a hadron is given by the symmetric Lund fragmentation function

$$f(z) = \frac{1}{z}(1-z)^a e^{-bm_T^2/z}, \tag{13}$$

where m_T is the transverse mass of the hadron an a and b are two parameters. In particular, this form implies that the heavier a hadron is, the larger an $E + p_L$ fraction will it take.

In the string model, gluons correspond to energy and momentum carrying kinks on the string spanned between a q and a $\bar{q}$ end. For a $q\bar{q}g$ system, e.g., the string is stretched from the quark via the gluon to the antiquark. Whereas a quark or antiquark thus has one string piece attached to it, a gluon has two, corresponding to the double colour charge of a gluon. In e^+e^- annihilation, the string and the independent fragmentation pictures predict rather different event structures, in particular for low-momentum particles. Evidence supporting the string picture was first observed by JADE, and has since been confirmed by several other groups.[40] Similar differences are predicted for hadron physics, but are much more difficult to study experimentally, and no conclusive evidence exists.

It should be noted that the free parameters of the fragmentation model have been determined entirely from e^+e^- data. Comparisons with hadron physics will therefore offer immediate tests of jet universality. In the string approach, this not only applies to high-p_T jets but also to beam jets. The structure of beam jets can therefore be adjusted only by modifying

the non-fragmentation components, like the details of multiple interactions.

Future Plans

There are two major revisions planned for the next version of PYTHIA (5.1). The first is the inclusion of massive matrix elements for the $2 \to 2$ hard subprocesses. This will remove the need for a lower cut-off in p_T of the hard scattering and allow the user to study phenomena like charm production at SPS energies or bottom production at S$\bar{\text{p}}$pS energies with more confidence as to the lower end of the p_T-spectrum. (At present, a preliminary version with massive matrix elements tailored for SPS energies exists as CHARIS and is being used by the LEBC-EHS Collaboration for comparisons with data.[41]) The second is the expansion of the program to allow also e^+e^- and ep in the initial configuration, which means that PYTHIA will mature into a multi-purpose program capable of handling questions in all major branches of high-energy physics, as behooves a true oracle.

Monte Carlo Files

The Lund Monte Carlo is available to all interested parties, and should be possible to run on any machine with a FORTRAN 77 compiler. The latest versions of the programs are available either on the Fermilab VAX cluster (DECNET node FNAL), under USR$ROOT1:[V3343], or on the UCLA VAX (DECNET node UCLA), under DRC1:[GOLLUM]. A DECNET user can thus access the source file for PYTHIA 4.7 by copying

FNAL::USR$ROOT1:[V3343]PYTHIA47.FOR or
UCLA::DRC1:[GOLLUM.HIGHPT]PYTHIA47.FOR.

The fragmentation routines of JETSET 6.2 can be copied from

FNAL::USR$ROOT1:[V3343]JETSET62.FOR or
UCLA::DRC1:[GOLLUM.FRAGMENT]JETSET62.FOR.

A manual of the program is available on the file

FNAL::USR$ROOT1:[V3343]PYTHIA47.MAN or
UCLA::DRC1:[GOLLUM.HIGHPT]PYTHIA47.MAN.

Users who want to run PYTHIA 4.7 with the structure function evolution program of Wu-Ki Tung should also copy the files

UCLA::DRC1:[GOLLUM.STRFUN]PYSTFU.FOR,
FNAL::USR$ROOT1:[ZAQ.PDFIIT]PSETUP_51.FOR,
FNAL::USR$ROOT1:[ZAQ.PDFIIT]PDFIT_51.FOR.

There is in addition an interactive demonstration program available on the file

UCLA::DRC1:[GOLLUM]PYDEMO47.FOR,

which can be linked with PYTHIA 4.7 and JETSET 6.2 (and the files for structure function evolution, if so desired) and run to familiarize the user with some of the major options available in PYTHIA 4.7. However, this last program is tailored for the VAX and might not work (without some slight revisions) on other machines. Files are also available on the Fermilab Cybers, but are not updated as frequently; check file README.LOG of user V3343 on FNAL or LUNDMC.MAN of user GOLLUM on UCLA for further information, last updates, etc. Questions regarding the program should be sent to DECNET address UCLA::GOLLUM or BITNET address IUY9GOL@UCLAMVS (H.-U. Bengtsson, UCLA), or BITNET address THEP@SELDC51 (T. Sjöstrand, Lund).

Conclusion

Having ascertained the truthfulness of the Pythia, Crœsus now sent a second embassy to Delphi inquiring after the outcome of a battle against the Persians and received the answer[42]

Κροῖσος Ἅλυν διαβὰς μεγάλην ἀρχὴν καταλύσει.

[*If Crœsus passes over the Halys he will dissolve a great empire.*]

Taking this to mean that he would conquer, the king of all Lydians entered into an alliance with Lacedæmones, Babylonians and Egyptians, and strengthened in confidence no less than in manpower he crossed into Cappadocia, only to be defeated and taken prisoner by Cyrus. When Crœsus then upbraided Apollo for having misled him, the god answered through his medium that he had correctly predicted the destruction of a great empire — Crœsus' own — and could not be held responsible if people chose to interpret his words after their own fashion. The moral of this story is obvious also when applied to Monte Carlo programs: the answers given may very well be correct, but they demand a careful interpretation.

Acknowledgements

Large fractions of the work described here have been carried out at SSC workshops. Our thanks therefore go to the organizers of the Snowmass 1984, Oregon 1985, UCLA 1986, Madison 1986 and Snowmass 1986 meetings. One of us (T. S.) would also like to thank the Fermilab theory group for their hospitality and the Swedish Natural Science Research Council for supporting visits to the US.

References

[1] Herodotus Halicarnasseus, *Historiarum Liber I (Clio)*, 47.
[2] H.-U. Bengtsson, Computer Phys. Comm. **31** (1984) 323.
[3] H.-U. Bengtsson, G. Ingelman, Computer Phys. Comm. **34** (1985) 251.
[4] H.-U. Bengtsson, T. Sjöstrand, in preparation.
[5] R. K. Ellis, J. C. Sexton, Nucl. Phys. **B269** (1986) 445. (1985).
[6] J. F. Gunion, Z. Kunszt, Phys. Rev. **D33** (1986) 665.
[7] W.-S. Hou, A. Soni, Phys. Rev. Lett. **54** (1985) 2083.
[8] K. Lane, in *Proceedings of the 1982 DPF Summer Study on Elementary Particle Physics and Future Facilities*, edited by R. Donaldson, R. Gustafson and F. Paige (Fermilab, Batavia, Illinois), p. 222.
J. F. Gunion, H. E. Haber, F. Paige, W.-K. Tung, S. S. D. Willenbrock, UC Davis preprint UCD-86-15 (1986).
[9] M. Dine, V. Kaplunovsky, M. Mangano, C. Nappi, N. Seiberg, Nucl. Phys. **B259** (1985) 549.
[10] E. Eichten, I. Hinchliffe, K. Lane, C. Quigg, Rev. Mod. Phys. **56** (1984) 579.
E. Eichten, I. Hinchliffe, K. Lane, C. Quigg, Fermilab preprint FERMILAB-Pub-86/75-T.
[11] B. Andersson, H.-U. Bengtsson, in preparation.
[12] G. Gustafson, Z. Physik **C15** (1982) 155.
[13] D. Duke, J. F. Owens, Phys. Rev. **D30** (1984) 49.
[14] M. Glück, E. Hoffman, E. Reya, Z. Physik **C13** (1982) 119.
[15] J. F. Owens, Phys. Rev **D30** (1984) 943.
[16] J. C. Collins, W.-K. Tung, Fermilab preprint FERMILAB-Pub-86/39-T (1986)
W.-K. Tung, Parton Distribution Functions Incorporating Heavy Quark Mass Effects, to be published in Proceedings of the Madison Workshop, May 5–16, 1986.
[17] H.-U. Bengtsson, W.-S. Hou, A. Soni, D. H. Stork, Phys. Rev. Lett. **55** (1985) 2762.
[18] M. M. Block, R. N. Cahn, Rev. Mod. Phys. **57** (1985) 563.
M. M. Block, Talk presented at XXIst Rencontre de Moriond, March 16–22, 1986.
[19] K. Goulianos, Phys. Rep. **101** (1983) 169.

[20] M. M. Block, R. N. Cahn, Phys. Lett. **149B** (1984) 245.
[21] J. F. Gunion, Z. Kunszt, Phys. Lett. **159B** (1985) 167.
S. J. Parke, T. R. Taylor, Nucl. Phys. **B269** (1986) 410.
S. J. Parke, T. R. Taylor, Fermilab preprint FERMILAB-Pub-85/162-T.
Z. Kunszt, Nucl. Phys. **B271** (1986) 333.
[22] T. D. Gottschalk, in *Supercollider Physics*, edited by D. E. Soper (World Scientific, Singapore, 1986), p.3.
[23] G. Altarelli, G. Parisi, Nucl. Phys. **B126** (1977) 298.
[24] K. Kajantie, E. Pietarinen, Phys. Lett. **93B** (1980) 269.
[25] G. C. Fox, S. Wolfram, Nucl. Phys. **B168** (1980) 285.
R. Odorico, Nucl. Phys. **B172** (1980) 157.
C.-H. Lai, J. L. Petersen, T. F. Walsh, Nucl. Phys. **B173** (1980) 141.
R. Kirschner, S. Ritter, Physica Scripta **23** (1981) 763.
T. D. Gottschalk, Nucl. Phys. **B214** (1983) 201.
[26] G. Marchesini, B. R. Webber, Nucl. Phys. **B238** (1984) 1.
[27] A. H. Mueller, Phys. Lett. **104B** (1981) 161.
B. I. Ermolaev, V. S. Fadin, JETP Lett. **33** (1981) 269.
A. Bassetto, M. Ciafaloni, G. Marchesini, Phys. Rep. **100** (1983) 201.
[28] T. Sjöstrand, Computer Phys. Comm. **39** (1986) 347.
[29] M. Bengtsson, T. Sjöstrand, in preparation.
[30] UA1 Collaboration, G. Arnison et al., CERN preprint CERN-EP/86-55 (1986).
[31] R. D. Field, G. C. Fox, R. L. Kelly, Phys. Lett. **119B** (1982) 439.
M. P. Shatz, Caltech thesis/preprint CALT-68-1145 (1984).
[32] R. Odorico, Nucl. Phys. **B228** (1983) 381.
R. Odorico, Computer Phys. Comm. **32** (1984) 139.
[33] T. Sjöstrand, Phys. Lett. **157B** (1985) 321.
[34] M. Bengtsson, T. Sjöstrand, M. van Zijl, Lund preprint LU TP 86-1 (1986), to appear in Z. Physik **C**.
[35] UA1 Collaboration, G. Arnison et al., Lett. Nuovo Cimento **44** (1985) 1.
UA2 Collaboration, J. A. Appel et al., Z. Physik **C30** (1986) 1.
[36] T. Sjöstrand, Fermilab preprint FERMILAB-Pub-85/119-T (1985).
[37] UA5 Collaboration, G. J. Alner et al., Phys. Lett. **138B** (1984) 304.
[38] T. Sjöstrand, Fermilab preprint FERMILAB-Conf-86/89-T (1986).
T. Sjöstrand, M. van Zijl, in preparation.
[39] B. Andersson, G. Gustafson, G. Ingelman, T. Sjöstrand, Phys. Rep. **97** (1983) 33.
[40] JADE Collaboration, W. Bartel et al., Phys. Lett. **101B** (1981) 129.
JADE Collaboration, W. Bartel et al., Z. Physik **C21** (1983) 37.
JADE Collaboration, W. Bartel et al., Phys. Lett. **157B** (1985) 340.
TPC Collaboration, H. Aihara et al., Z. Physik **C28** (1985) 31.
TASSO Collaboration, M. Althoff et al., Z. Physik **C29** (1985) 29.
Mark II Collaboration, P. D. Sheldon et al., SLAC preprint SLAC-Pub-4030 (1985).
[41] H.-U. Bengtsson, CHARIS - The Lund Monte Carlo for Charm Production, in preparation.
LEBC-EHS Collaboration, M. Aguilar-Benitez et al., Phys. Lett. **161B** (1985) 400.
LEBC-EHS Collaboration, M. Aguilar-Benitez et al., Phys. Lett. **164B** (1985) 404.
[42] Diodorus Siculus, *Bibliotheca Historica, Fragmenta Libri IX*, 31.